Advanced Estimation Techniques of Road Surface Condition and Their Experimental Evaluation using Test Electric Vehicle "UOT March I and II"

Kimihisa Furukawa
Department of Electrical Engineering The University of Tokyo
Ce-503, 4-6-1 Komaba, Meguro, Tokyo 153-8505 Japan
Tel: +81-3-5452-6289, Fax: +81-3-5452-6288, E-mail: furukawa@horilab.iis.u-tokyo.ac.jp

Yoichi Hori
Institute of Industrial Science The University of Tokyo
Ce-501, 4-6-1 Komaba, Meguro, Tokyo 153-8505 Japan
Tel: +81-3-5452-6287, Fax: +81-3-5452-6288, E-mail: hori@iis.u-tokyo.ac.jp, y.hori@ieee.org

Abstract

In this paper, advanced techniques of road surface condition estimation for electric vehicles (EVs) are reported. Information on driving-force transmitted from the tire to the road is indispensable for the estimation of road surface condition in deciding a vehicle's state of motion. In our laboratory, various road surface condition estimation techniques have been proposed based on driving-force observer. This observer utilize one of the excellent features of EVs, i.e., motor torque can be known easily and precisely from motor current. First, the principle of the driving-force observer is explained. Next, two kinds of the road surface condition estimation techniques are introduced. One is μ_{peak} and λ_{opt} estimation techniques and μ-λ curve information. The other is based on vibration characteristics without vehicle velocity. Finally, applications of these estimation techniques are shown and confirmed experimentally using the test EVs "UOT March I and II".

Keywords: Electric Vehicle, Wheel Hub Motor, Traction Control, Road Surface Condition Estimation, Driving-Force, Slip Ratio, Frictional Coefficient

1 Introduction

In these days, Electric Vehicles (EVs) attract attention as one of environment-friendly technologies. However, researches on motion control for EVs are not so well developed, although it can utilize the most remarkable merit of electric motor [1][2][3][4].

We have pointed out the following three advantages of EVs:
1. Motor torque can be known easily and precisely from motor current.
2. Motor torque generation is very quick and accurate.
3. Motor can be installed in each wheel.

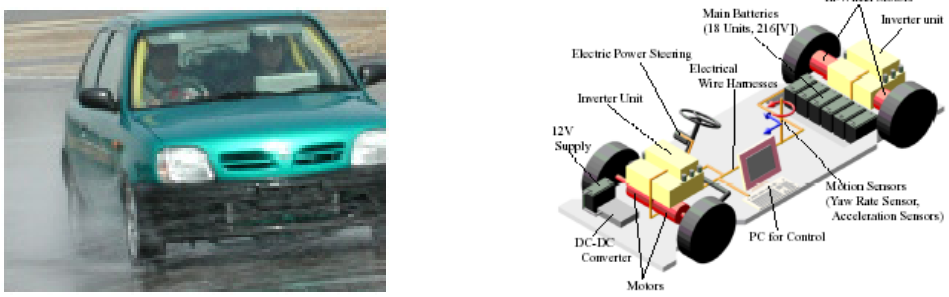

Figure 1: Our handmade Experimental EV "UOT March II"

In our laboratory, many researches to utilize these merits of EVs are performed and verified by the experimental EVs "UOT (University of Tokyo) March I and II".

UOT March II can be used for two-dimensional motion control experiment (Figure 1). A wheel hub motor is installed in each wheel, and the torque of each wheel can be controlled with full independence [2][3][5]. In this paper, road surface condition estimation techniques are introduced using the advantage of 1 [6]. The road surface condition estimation is an important technique for active safety systems. In past researches, it is well known that driving-force between tire and road has significant information. For Internal Combustion Vehicles (ICVs), direct estimation is impossible using driving-force information because observation of generated engine torque is difficult. On the contrary, in the case of EVs, the estimation using driving-force observer is possible because it is easy to monitor generated motor torque.

Next, the road surface condition estimation techniques and their experimental results with "UOT March I " are shown. Section 2 describes frictional characteristics between tire and road. In section 3, the driving-force observer, which is utilizing the advantage of EVs, is introduced. In section 4, two kinds of road surface condition estimation techniques are introduced. First, μ_{peak} and λ_{opt} estimation techniques based on characteristics of μ-λ curve are introduced in 4.1. Second, a novel estimation technique based on the vibratory characteristics is proposed and investigated in 4.2. This technique utilizes only driving force and wheel velocity without chassis velocity. In section 5, applications of the road surface condition estimation techniques are shown.

2 Frictional characteristics between tire and road

In this section, frictional characteristics between tire and road are shown which are the fundamental concepts of the road surface condition estimation [7][8]. Driving-force is generated by velocity difference between vehicle and wheel, i.e., the slip velocity. Vehicle behavior is decided by driving-force F_d shown in Figure 2. As shown in (1) driving-force is given by using frictional coefficient μ and normal force N.

$$F_d = \mu(\lambda)N \tag{1}$$

Frictional coefficient μ is the function of slip ratio λ shown in Figure 2, and this curve is called μ-λ curve. Slip ratio is given by using chassis velocity V and wheel velocity V_w as (2).

$$\lambda = \frac{V_w - V}{\max(V, V_w)} \tag{2}$$

The performance of driving-force is affected by the relationship between μ and λ, which has non-linear characteristics with peak value μ_{peak} (hereinafter referred to as peak frictional coefficient). The slip ratio λ_{opt} (hereinafter referred to as optimal slip ratio) where frictional coefficient has μ_{peak} is usually from 0.05 to 0.2.

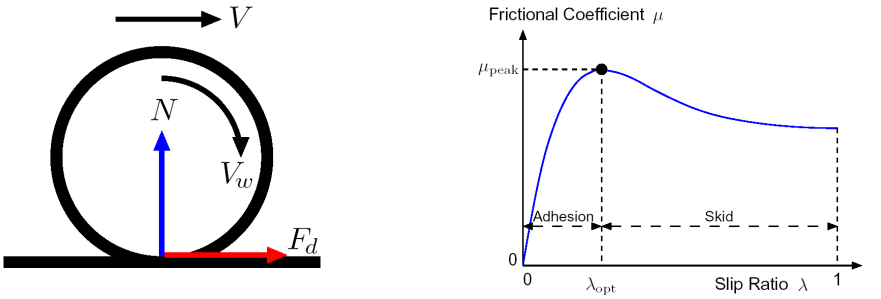

(a) Driving force between tire and road in one wheel model

(b) Characteristics of μ-λ curve

Figure 2: The schematic of one wheel model and the characteristic illustration of μ-λ curve

In adhesion state: $\lambda \le \lambda_{opt}$, vehicle is in stable because the condition between tire and road is in adhesive. In skid state: $\lambda > \lambda_{opt}$, the wheel is accelerated and big spin occurs. The road surface condition estimation is used for the purpose of holding vehicle motion stable. In other words, it estimates the stability limit between adhesion and skid states when the vehicle is in adhesion.

3 Driving-force observer

The information of frictional coefficient μ is indispensable for road surface condition estimation. As it was shown in (1), frictional coefficient is obtained by driving-force F_d and normal force N. However it is impossible to observe directly driving-force generated between tire and road, therefore observer is needed to estimate driving-force. In this section, the principle of driving-force observer is briefly explained [9].

In electric motor, generated torque can be monitored precisely and easily, therefore it is possible for EVs to estimate driving-force with high precision. In the case of EVs, motor current and wheel velocity, which are needed to calculate generated torque, can be measured. Actually, armature current in a DC motor or torque current in an AC motor is used. The dynamic equations about a driving wheel and a chassis, (3), are derived from one wheel vehicle model shown in Figure 3,

$$M_w \frac{dV_w}{dt} = F_m - F_d, \quad M\frac{dV}{dt} = F_d \tag{3}$$

where, M_w is wheel inertia converted to mass, F_m is motor torque converted to force, F_d is driving-force and M is vehicle body mass. The dynamic equation of driving wheel shown in (3) is used to derive driving-force as (4),

$$F_d = \frac{1}{r}(T - J\frac{d\omega}{dt}) \tag{4}$$

where, r is radius of wheel, T is motor torque, J is wheel inertia and ω is angular velocity of driving wheel. These values are related with F_m, M_w, and V_w respectively as follows.

$$F_m = T/r, \quad M_w = J/r^2, \text{ and } V_w = r\omega \tag{5}$$

Based on (4), the block diagram of the driving-force observer is shown in Figure. 4. The figure is for a shunt DC motor case, $\hat{F}_d$, K, N, and J_n are the estimated driving-force, the torque coefficient, the gear ratio of transmission, and the nominal value of wheel inertia respectively. This is called driving-force observer, though this structure is the same as disturbance observer often used in mechatronics. The observer uses first order derivative of ω, which induces higher frequency noise from differential operation. Therefore, low pass filters "Q" are needed.

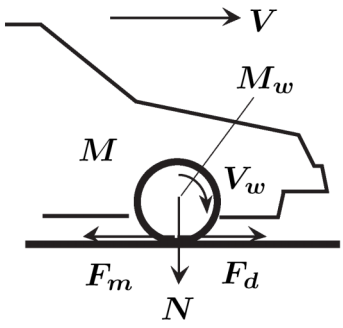

Figure 3. The schematic of one wheel vehicle model

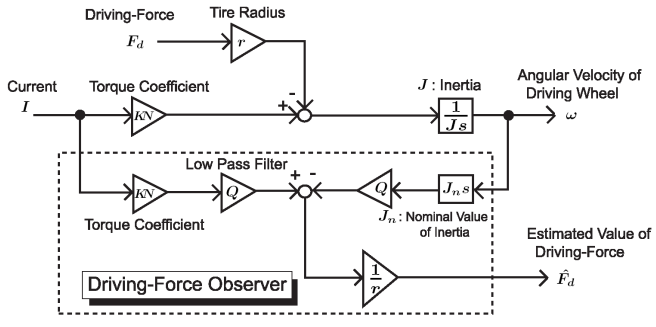

Figure 4. Block diagram of the driving-force observer

4 Road surface condition estimation using driving-force observer

The road surface condition estimation based on the driving-force observer is one of the merits of EVs. In this section, the road surface condition estimation techniques for EVs are introduced.

4.1. Estimation techniques using μ -λ relation

4.1.1. μ_{peak} estimation based on tire brush model

The tire model proposed by Dr. Yamazaki says that the value of $d\mu/d\lambda$ (hereinafter referred to as μ gradient) includes the information of peak frictional coefficient μ_{peak} [10]. Therefore, the value of μ_{peak} can be estimated by the data of driving-force, wheel velocity, chassis velocity and typical characteristics of μ-λ curve. This technique is very useful to prevent big skidding [6]. First, a physical analysis about the frictional characteristics between tire and road is given. On tire tread, adhesive and sliding areas are mixed. The proportion of two areas is changed by the slip ratio as shown in Figure 5(a).

This phenomenon is analyzed based on the brush model (see Figure 5(b)). The distribution of ground contact pressure in tire tread is assumed as parabolic shape shown in Figure 5(c). Ground contact pressure p is given as (6) using maximum ground contact pressure p_m, and ground contact length, l.

$$p = 4p_m \frac{\xi}{l}\left(1-\frac{\xi}{l}\right) \tag{6}$$

Normal force of tire tread, N, is given by (7) using ground contact width.

$$N = \frac{2}{3} p_m w l \tag{7}$$

In adhesive area, friction stress $\sigma_\xi^{(a)}$ is decided by shearing stress and use longitudinal spring constant of tread rubber for each unit area. In sliding area, friction stress $\sigma_\xi^{(s)}$ is decided by peak frictional coefficient μ_{peak}. They are given by (8).

$$\sigma_\xi^{(a)} = k_x \lambda \xi, \quad \sigma_\xi^{(s)} = \mu_{peak} p \tag{8}$$

The friction stresses take the same value at the boundary between adhesive and sliding areas represented by $\xi = a$,

$$\sigma_a^{(a)} = \sigma_a^{(s)}. \tag{9}$$

Driving-force F_d is given by (10),

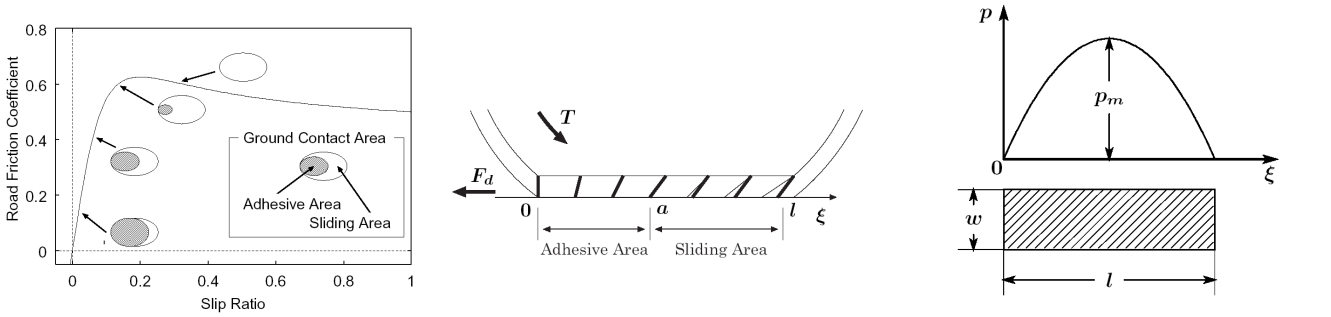

(a) Variation of adhesive and sliding areas (b) Tire brush model (c) Distribution of ground pressure

Figure 5: Physical configurations of tire tread

$$
\begin{aligned}
F_d &= \int_0^l \sigma_\xi w d\xi \\
&= \int_0^a \sigma_\xi^{(a)} w d\xi + \int_a^l \sigma_\xi^{(s)} w d\xi \\
&= C_s\lambda - \frac{(C_s\lambda)^2}{3\mu_{peak}N} + \frac{(C_s\lambda)^3}{27(\mu_{peak}N)^2}
\end{aligned} \tag{10}
$$

where, driving stiffness C_s, which is the driving-force for unit slip ratio at $\lambda = 0$, is given by (11).

$$
C_s = \frac{1}{2} w k_x l^2 \tag{11}
$$

The solution of the maximum driving-force, $\mu_{peak}N$, from (10) is obtained as (12).

$$
\mu_{peak}N = \frac{3(C_s\lambda)^2 + \sqrt{3(C_s\lambda)^3(4F_d - C_s\lambda)}}{18(C_s\lambda - F_d)} \tag{12}
$$

As measured signals contain much noise, μ_{peak} estimation is difficult if (12) is directly applied. To identify linear characteristics represented by (13), algorithm of adaptive identification (recursive least-squares (RLS) method) is applied,

$$
y[k] = \hat{\theta}^T[k]\phi[k] \tag{13}
$$

where, $y[k]$, $\phi[k]$ and $\theta[k]$ take the forms of (14).

$$
y[k] = 3(C_s\lambda)^2 + \sqrt{3(C_s\lambda)^3(4F_d - C_s\lambda)}\ , \quad \hat{\theta}[k] = \mu_{peak}N, \quad \text{and} \quad \phi[k] = 18(C_s\lambda - F_d) \tag{14}
$$

In the case of Fixed Trace (FT) method, trace gain $\gamma = trP[k]$ is fixed. Especially, in the 1st dimension FT method, forgetting factor κ is given by (15),

$$
\kappa = \frac{1}{1 + \gamma\left\|\phi[k]\right\|^2}\ . \tag{15}
$$

In comparison with RLS, FT method uses variable forgetting factor κ because trace gain $\gamma = const.$ as (15). In other words, when $\phi[k]$ is big and $\hat{\theta}$ can be identified with good precision, $\hat{\theta}$ is updated in a short time. Whereas, when $\phi[k]$ is small and not of "rich" information, $\hat{\theta}$ is seldom updated.

To confirm the validity of the introduced technique, road surface condition is estimated in off-line calculation using the data measured by the experimental EV "UOT March I". The experimental data in dry asphalt road and the estimation result of maximum driving-force are shown in Figure 6. In this experiment, the vehicle is accelerated at 2 sec. Hence, slip ratio grows bigger immediately by urgent acceleration.

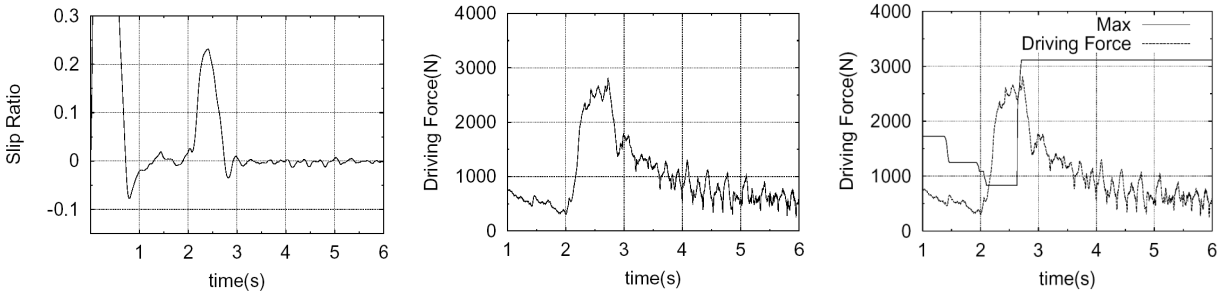

Figure 6: Experimental data on asphalt road and result of the μ_{peak} estimation

4.1.2. λ_{opt} estimation based on geometric similarity of μ - λ curve

To estimate the optimal slip ratio, λ_{opt}, we use the information of μ, λ and μ gradient. However, this information contains much noise and error, too, stable estimation is difficult in search algorithm such as gradient method. In this section, as a robust optimal slip ratio estimation Fuzzy inference is introduced [8]. One of the characteristics of the μ-λ curve, optimal slip ratio λ_{opt} has strong relation with μ gradient (see Figure 7, A_1 and A_2 represent μ gradient). This geometrical characteristic can be applied to λ_{opt} estimation. This characteristic is proved in μ-λ curves which have same μ_{peak}. We do not need so accurate μ_{peak} value. Then, we need similarity information of μ_{peak} with four kinds of standard road surface conditions, ASPHALT, GRAVEL, SNOW and ICE, which are displayed in Figure 8. Using μ and λ values, degrees of similarity to the standard road surface conditions are obtained numerically by Fuzzy inference.

In optimal slip ratio estimation, we need two kinds of algorithms. The first algorithm is to obtain road surface condition similarities with four kinds of standard road surface conditions, described as above. The second algorithm is λ_{opt} estimation to the standard road surface conditions with Fuzzy inference. This estimation uses estimated μ gradient: $\hat{A}$, and λ based on geometrical characteristics.

The block diagram of the optimal slip ratio estimator is shown in Fig. 9. Using information from these algorithms, $\hat{\lambda}_{opt}$ is obtained by (16). Estimated optimal slip ratios to each standard road, $\hat{\lambda}_{opt_A}$, $\hat{\lambda}_{opt_G}$, $\hat{\lambda}_{opt_S}$, and $\hat{\lambda}_{opt_I}$ are weighted by K_A, K_G, K_S, and K_I respectively, which are road surface condition similarities with standard road surface conditions.

$$\hat{\lambda}_{opt} = \frac{K_A \hat{\lambda}_{opt_A} + K_G \hat{\lambda}_{opt_G} + K_S \hat{\lambda}_{opt_S} + K_I \hat{\lambda}_{opt_I}}{K_A + K_G + K_S + K_I} \tag{16}$$

The estimated result by this technique will be shown in 5.2.

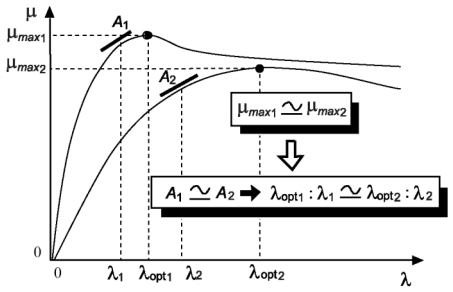

Figure 7: Geometrical characteristics of μ-λ curves

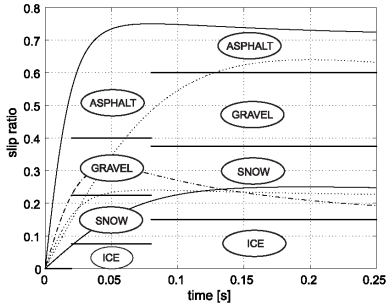

Figure 8: The schematic about the classification of road surface conditions

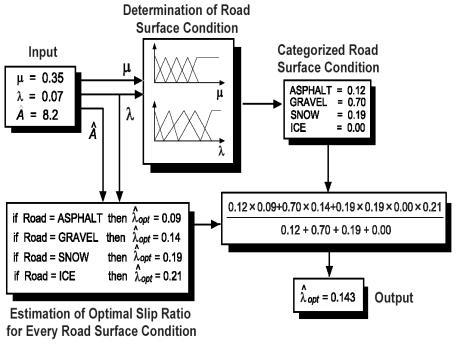

Figure 9: Block diagram of optimal slip ratio estimator

4.2. Proposal of a novel estimation technique based on vibration characteristics

The road surface condition estimation techniques based on the information of slip ratio and driving-force were described in the previous sections. These techniques need chassis velocity to obtain slip ratio. The novel estimation technique proposed in this section uses vibration characteristics between driving-force and wheel velocity. It does not need chassis velocity. In the following, this estimation technique is introduced by using the experimental data from "UOT March I", and its effectiveness is confirmed.

The block diagram of the road surface condition estimation is shown in Figure 11. In this estimation technique, a system transfer characteristic from wheel velocity to driving-force is analyzed by using the experimental data. To analyze the road condition change, Short Time Fourier Transform (STFT) is utilized.

As is well known, the original Fourier Transform takes the form of (17).

$$X(e^{j\omega}) = \sum_{n=-\infty}^{\infty} x(n)e^{-j\omega n} \tag{17}$$

On the other hand, STFT is given by (18).

$$X_{kn}(e^{j\omega}) = \sum_{n=-\infty}^{\infty} x(n)w(n-kN)e^{-j\omega n} \tag{18}$$

When we need to detect the change of the frequency spectrum according to time, the signal $x(n)$ with the window function $w(n)$ and limited length N_w is calculated by the Fourier transform. The signal $x(n)$ is cut out by the window function $w(n)$ and this is the reason why this calculation is called Short Time Fourier Transform. The window function is shifted along time axis. Above-mentioned procedure is repeated to analyze the time dependent frequency spectrum. The concept of the signal processing is shown in Figure 11. By using STFT, the time shift of system transfer function can be observed. When the system input and output are assumed to be $x(n)$ and $y(n)$ respectively, the transfer function $G(j\omega)$ is given by (19),

$$P_{xy}(j\omega) = G(j\omega)P_{xx} \tag{19}$$

where, the auto-correlation function R_{xx} and the cross-correlation function R_{xy} are defined by (20).

$$R_{xx}(m) = E\{x(n)x^*(n+m)\},\quad R_{xy}(m) = E\{x(n)y^*(n+m)\} \tag{20}$$

Then, the power spectrum density: $\hat{P}_{xx}(j\omega)$, $\hat{P}_{xy}(j\omega)$ and the transfer function: $\hat{G}(j\omega)$ are obtained as follows:

$$\hat{P}_{xx}(j\omega) = \sum_{m=-\infty}^{\infty} R_{xx}(m)e^{-j\omega m},\quad \hat{P}_{xy}(j\omega) = \sum_{m=-\infty}^{\infty} R_{xy}(m)e^{-j\omega m},\quad \text{and}\quad \hat{G}(j\omega) = \frac{\hat{P}_{xy}}{\hat{P}_{xx}}. \tag{21}$$

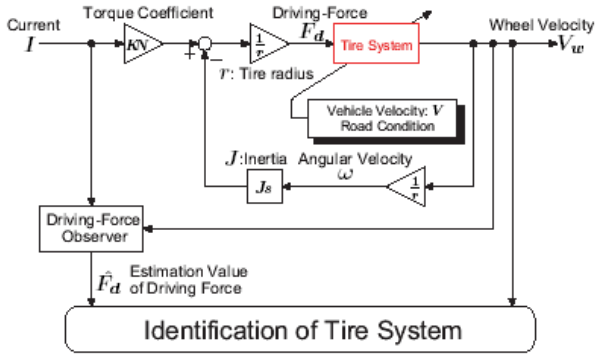

Figure 10: Block diagram of tire system identification

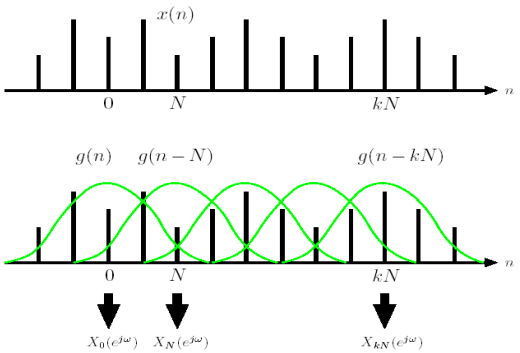

Figure 11: STFT analysis

These relations are applied to the experimental data and the frequency spectrum of transfer function from wheel velocity $x(n) = V_w$ to driving-force $y(n) = F_d$ is analyzed. The experimental condition is shown in Figure 12. We used wet iron plates as slippery road surface. Water is scattered to reduce the friction coefficient. The front wheels are on the wet iron plate area between $t = 1.3$ sec. and 2.0 sec. In the analysis, Hanning window shown in Figure 13 is applied. The experimental data and the result of the analysis are shown in Figures 14 and 15, respectively. As the result of this analysis, the transfer function gain on wet plate is bigger than that on dry asphalt road. This characteristic appears around 10Hz or less.

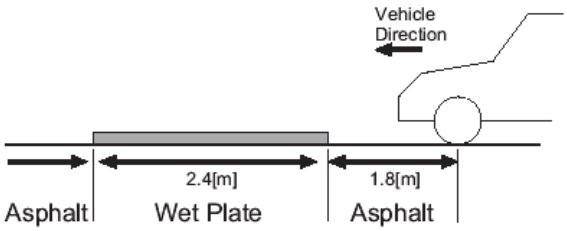

Figure 12: Road condition in experiment

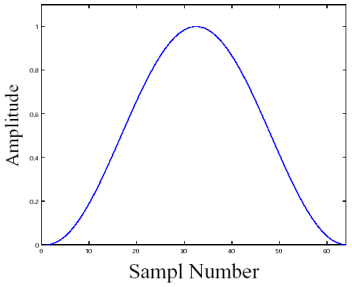

Figure 13: STFT analysis

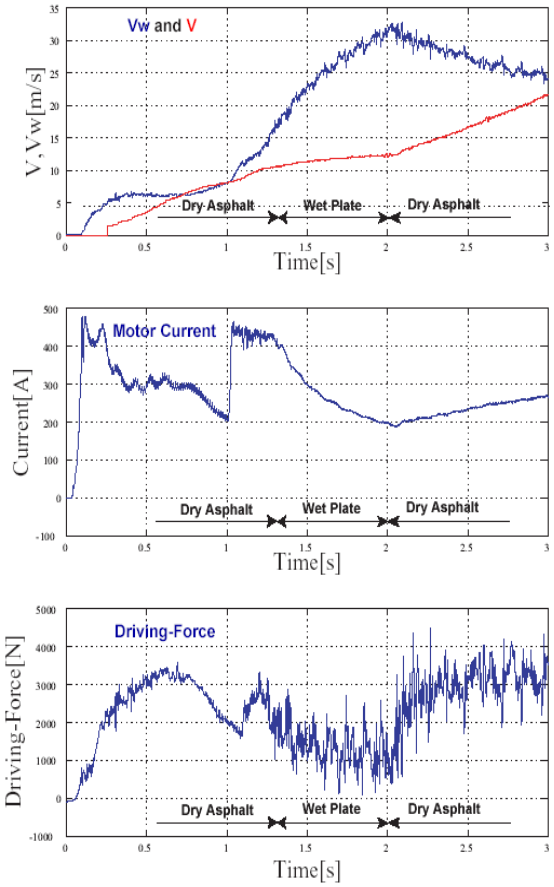

Figure 14: Experimental data

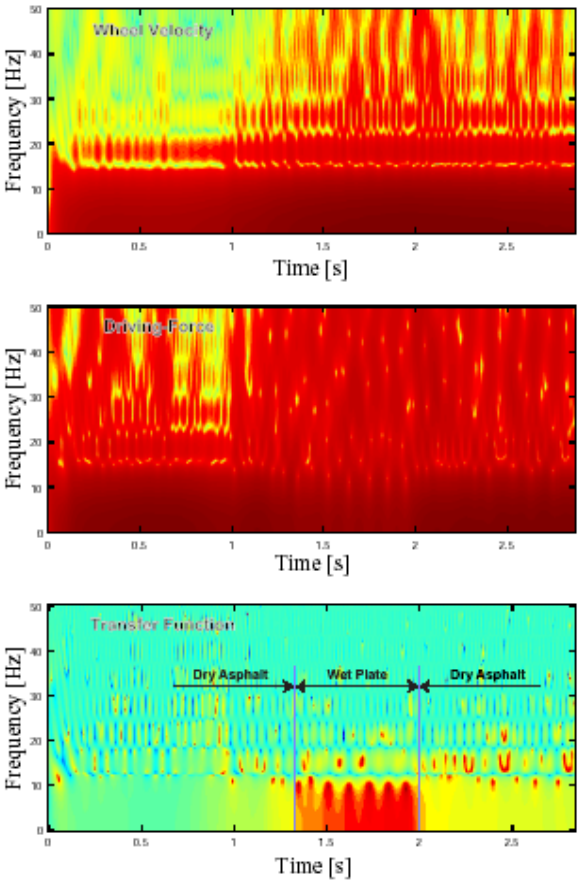

Figure 15: Result of STFT analysis

5 Application of the road surface condition estimation

5.1. Indication of adhesion rate to driver

If the car tells the driver "Our car has entered snowy road", it must be a great help for vehicle safety. The μ_{peak} estimation technique realizes this function [6].

The technique for μ_{peak} estimation before entering skid state was proposed in 4.1.1. The ratio of present driving-force to estimated maximum driving-force can be used as the information of adhesion state between tire and road. The adhesion rate r is defined as (22).

$$r = \frac{F_d}{\mu_{peak} N} \tag{22}$$

In (22), F_d and $\mu_{peak} N$ are obtained by the driving-force observer and peak frictional coefficient estimator respectively.

Adhesion state between tire and road can be quantitatively presented to driver by showing r. In the case that r is low, the state of tire is kept in adhesive if wheel is accelerated further more. Meanwhile, in the case that r approaches 1, the possibility of skidding is high even if wheel is accelerated a little.

Driving-force and adhesion rate when vehicle runs from dry asphalt road to wet iron plate suddenly is shown in Figure 16. On dry asphalt road, r is about 0.5 and the vehicle is in safe state. While, on wet iron plate, r is rapidly up to about 0.8 shown in Fig. 16(b). It is possible to inform quantitatively how easy to skid caused by sudden change in road surface condition even if the driving-force is kept almost constant as shown in Figure 16(a).

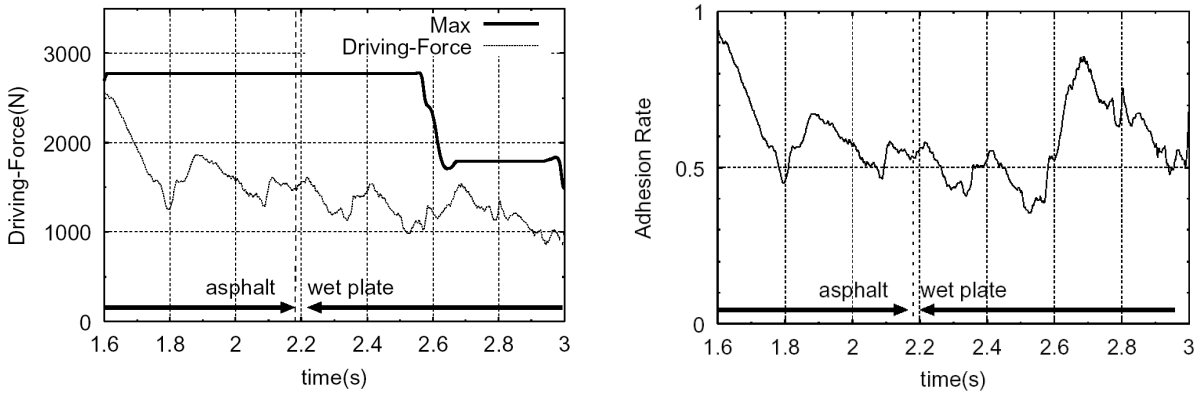

(a) Estimated maximum driving-force (b) Indicated adhesion rate

Figure 16: Estimation result of driving-force and adhesion rate when road surface condition changes Suddenly

5.2. Optimal slip ratio control

Slip ratio can be maintained to commanded value by strong feedback control. As driving-force is affected by highly nonlinear frictional characteristics between tire and road, real-time generation of optimal slip ratio is necessary while vehicle is moving (see 4.1.2).

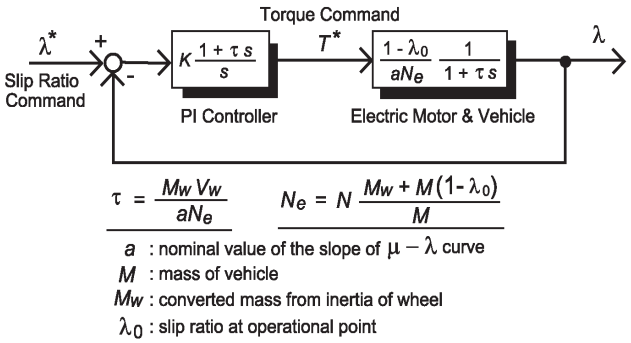

Figure 17: Block diagram of slip ratio control

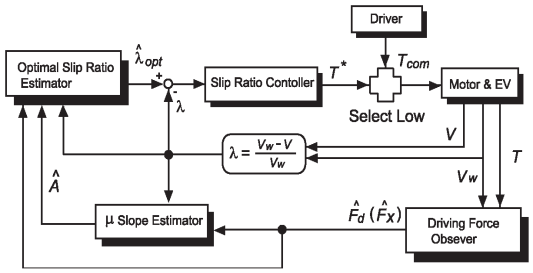

Figure 18: Whole block diagram of the optimum slip ratio control system

The technique of optimal slip ratio control, which makes λ follow up λ_{opt} changing in real-time with road surface condition, realizes the maximization of driving-force. To achieve this control, slip ratio control shown in Figure 17 is applied. $\hat{\lambda}_{opt}$, the estimated λ_{opt} using the optimal slip ratio estimator, is set up as the desired value for the slip ratio control. To obtain $\hat{\lambda}_{opt}$, the estimation algorithm based on Fuzzy inference is applied, introduced in 4.1.2. The whole block diagram of the optimal slip ratio control system is shown in Figure 18 [8].

Here, cruising simulation is performed using the estimation algorithm explained in 4.1.2. The approximated Magic-Formula shown in (23) is applied for μ-λ curve.

$$\mu = C\sin(D\arctan(E\lambda)) \tag{23}$$

Five μ-λ curves which have different μ_{opt} and λ_{opt} are decided by using the experimental data from "UOT March I" for the simulation. These curves are shown in Figure 19.

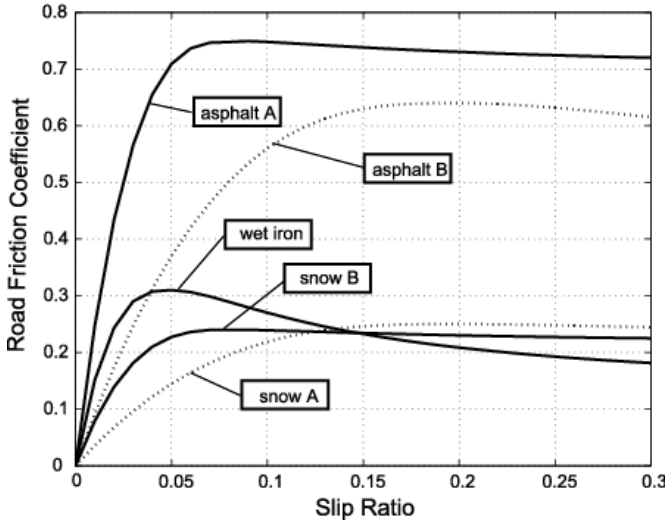

Figure 19: The schematic of μ-λ curves used in simulation

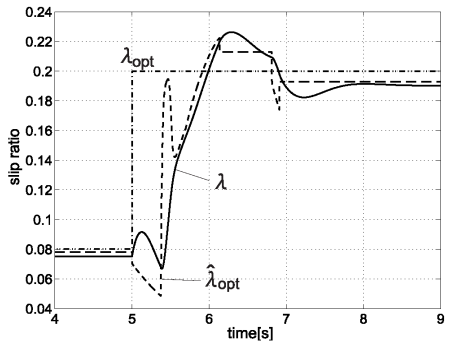

(a) Change from asphalt A to asphalt B

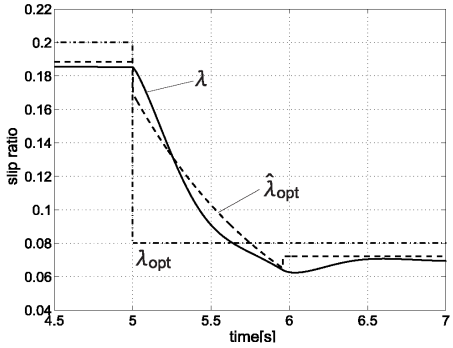

(b) Change from asphalt B to asphalt A

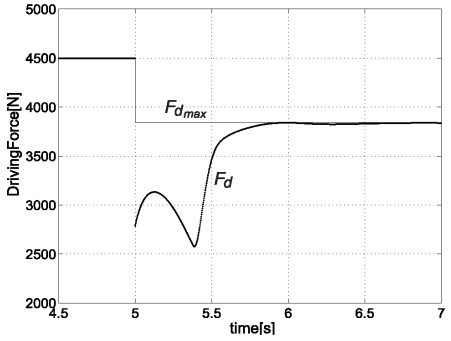

(c) Change of driving-force in case of (a)

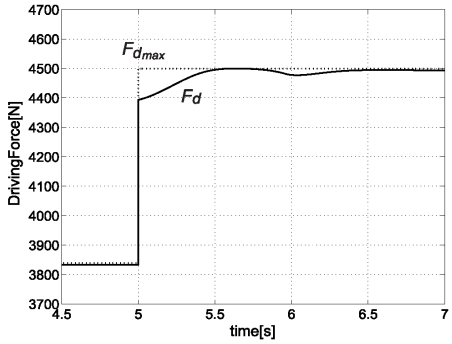

(d) Change of driving-force in case of (b)

Figure 20: Simulation results at the changing road surface condition

Transient response of λ is simulated in the case that vehicle is in full acceleration and the frictional characteristic changed at the moment of 5 sec. Dead-zone is set in $-0.1 < \hat{A} < 0.5$, and Low Pass Filter is inserted into λ and μ to uniform the delay of input signals to each estimator. Figures 20(a) and (b) are the estimation results when the road surface condition changes. It takes about 2 sec. to follow up in both case of Figs. 20(a) and (b).

Change in the driving-force of Figures 20(a) and (b) cases is depicted in Figures 20(c) and (d). The maximum driving-force is well followed within about 1 sec. This delay is allowable when slippery road, such as snow-covered road, continues for a long time, although it is difficult to estimate a small water pool suddenly appears during cruising even on asphalt road.

6 Conclusion

In this paper, the road surface condition estimation based on the driving force observer and some of its applications were given. As the examples of road condition estimation, μ_{peak} estimation based on Yamazaki's brush model of tire, λ_{opt} estimation based on geometric similarity of μ-λ curves, and a novel estimation technique based on vibration characteristics with Short Time Fourier Transform have been explained. As the applications, the indication technique of the adhesion rate to driver, and the optimal slip ratio control were given. These techniques can be realized firstly by using such advantages of electric motors that the motor torque can be known easily from the motor current. In other words, these advanced estimation and control techniques are only available in EV. We believe that these remarkable advantages of EV will open the new field of control and estimation in the future electric vehicle.

7 References

[1] Y. Hori, “Recent Trends of Electric Vehicle Technology”, Japan-China Bilateral Seminar on Transportation Research and Infrastructure Planning in 1998 (JC-TRIP’98), Beijing, 1998.

[2] Y. Hori, “Future Vehicle driven by Electricity and Control -Research on 4 Wheel Motored UOT March II”, Proc. of AMC 2002, invited paper, pp.1-14, Maribor, Slovenia, 2002.

[3] S. Sakai, H. Sado and Y. Hori, “Motion Control in an Electric Vehicle with Four Independently Driven In-Wheel Motors”, IEEE Trans. on Mechatronics, Vol.4, No.1, pp.9-16, 1999.

[4] H. Shimizu, K. Kawakami, Y. Kakizaki, S. Matsugaura and M. Ohnishi, ““KAZ” The super electric vehicle”, Proc. of EVS18, Berlin, 2001.

[5] S. Sakai, T. Okano, C. H. Tai, T. Uchida and Y. Hori, “4 Wheel Motored Vehicle “UOT Electric March II” -Experimental EV for Novel Motion Control Studies-”, INTERMAC2001 Joint Technical Conference, Tokyo, 2001.

[6] Y. Hori and K. Furukawa, “Road Surface Condition Estimation and Control utilizing Advantages of Electric Vehicle”, 27th Technical Meeting of Control Technology Division, 2nd Symposium of Adaptive and Learning Committee, SICE (Society of Instrumentation and Control Engineers), pp.1-16, 2002, in Japanese.

[7] Y. Hori, Y. Toyoda and Y.Tsuruoka, “Traction Control of Electric Vehicle -Basic Experimental Results using the Test EV UOT Electric March”, IEEE Trans. on Industry Applications, Vol.34, No.5, pp.1131-1138, 1998.

[8] H. Kataoka, H. Sado, S. Sakai and Y. Hori, “Optimal Slip Ratio Estimator for Traction Control System of Electric Vehicle based on Fuzzy Inference”, The Transactions of The Institute of Electrical Engineers of Japan, Vol.120-D, No.4, pp.581-586, 2000, in Japanese.

[9] H. Sado, S. Sakai and Y. Hori, “Road Condition Estimation for Traction Control in Electric Vehicle”, in Proc. of the 1999 IEEE International Symposium on Industrial Electronics, Bled. Slovenia, 99TH8465,Vol.2, pp.973-978, 1999.

[10] S. Yamazaki, “Evaluation of Friction Coefficient between Tire and Road Surface during Running”, Journal of Automotive Engineers of Japan, Vol.51, No.11, pp.58-62, 1997, in Japanese.

[11] K. Furukawa and Y. Hori, “Recent Development of Road Condition Estimation Techniques for Electric Vehicle and their Experimental Evaluation using the Test EV “UOT March I and II””, Proc. of IECON 2003, invited paper, Roanoke, Virginia, USA, 2003, to be presented.

8 Authors

Furukawa Kimihisa, Master's degree candidate, University of Tokyo, was born in 1978. He received B.C. degree in electrical engineering from Science University of Tokyo in 2002, and entered the master course in University of Tokyo. His research field covers power electronics, and motion control of electric vehicles. He is a member of the Institute of Electrical Engineers of Japan.

Yoichi Hori, received the B.S., M.S. and Ph.D degrees in Electrical Engineering from the University of Tokyo in 1978, 1980 and 1983, respectively. In 1983, he joined the University of Tokyo, the Department of Electrical Engineering as a Research Associate. He later became an Assistant Professor, an Associate Professor, and in 2000 a Professor. In 2002, he moved to the Institute of Industrial Science, the University of Tokyo, as a Professor of Information & System Division, Electrical Control System Engineering. During 1991-1992, he was a Visiting Researcher at the University of California, Berkeley (UCB). His research fields are control theory and its industrial application to motion control, mechatronics, robotics, electric vehicle, etc. He is now the Vice President of IEE-Japan IAS.